THE JOURNAL OF PHYSICAL CHEMISTRY B

Article

pubs.acs.org/JPCB

Role of Differential Transport in an Oscillatory Enzyme Reaction

Tamás Bánsági, Jr.* and Annette F. Taylor

School of Chemistry, University of Leeds, Leeds, LS2 9JT, U.K.

ABSTRACT: As a result of the bell-shaped pH-rate characteristic of enzymatic processes, feedback may arise in enzyme reactions having non-neutral products. This special type of product activation has been shown to lead to self-sustained pH oscillations in an enzyme-loaded membrane. We investigate the possibility of oscillations in a model of the urea−urease reaction, prompted by the recent experimental discovery of feedback in this reaction. An open system is considered in which acid and urea are transported to a cell containing the enzyme. Using linear stability analysis we determine the range of transport coefficients limit cycles may exist for and show that differential transport is required for oscillations in a class of compartmentalized enzyme processes similar to the urea−urease system. We demonstrate that although the transport rate of acid (k_H) must be greater than that of urea (k_S) for oscillations in a urease-loaded membrane, bistability is possible for $k_S \geq k_H$.

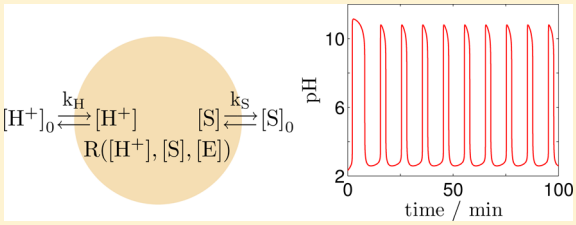

1. INTRODUCTION

Enzymatic processes are indispensable for sustaining life as maintaining a variety of functions in living organisms requires thousands of chemical transformations to be run at a high rate and selectivity. Biological cells rely on enzymes to achieve this by sufficiently lowering the energy barrier separating the reactant, or substrate, and product molecules of metabolic reactions. Enzymes are sensitive to their environment and have specific ranges of activity. Because of their strong amphoteric character, resulting from containing a large number of acid and basic groups, one of the most important factors affecting enzyme activity is pH. The rate of an enzymatic process typically follows a bell-shaped pH curve with the peak corresponding to maximum activity. When the product of the enzyme-catalyzed reaction is acidic or basic, this characteristic has been proposed to lead to oscillatory behavior in enzyme-loaded membranes,[1−5] supported by sparse experimental evidence.[6−8]

The number of enzymes proposed to give rise to oscillatory behavior has not significantly changed since the 1970s.[9] Theoretical and numerical studies focusing on feedback through acid have been mainly concerned with enzymes such as papain[1,10−12] and several others.[10,11,13,14] The oscillations in pH that occur in plants,[15] during glycolysis in yeast cells,[16] and by *Caenorhabditis elegans* for muscle contraction[17] are thought to be driven by other product-activated enzymes such as phosphofructokinase. Urease, however, despite an early experimental investigation in 1917 by Temminck Groll[7] that found damped oscillations in soybean extract, has not been discussed among the enzymes anticipated to produce oscillations. Urease is produced by a large number of plants, funghi and micro-organisms, and is a virulence factor for bacteria including *Helicobacter pylori* which has been linked to the development of stomach ulcers.[15,18] The urease-catalyzed hydrolysis of urea produces the base ammonia which raises the pH thereby protecting the bacteria from the harsh acidic environment of the stomach.

The urea−urease reaction follows Michaelis−Menten kinetics and has a bell-shaped rate−pH curve with maximum at pH 7. Recent studies presenting evidence of bistability in a flow reactor[19] and propagating pH fronts in a spatially distributed system[20] prompted us to examine the possibility of oscillations in this reaction. Using a model derived from earlier work, here we determine a physically reasonable range of parameter values for which oscillatory behavior might be observed in a urease-containing cell/membrane immersed in substrate solution or in an open reactor. In previous studies,[1,3,10−13] transport or diffusion coefficients of the substrates were considered constant, and therefore, their ratio was always fixed. By relaxing these restrictions, although not accounting for membrane charge, salt, and buffer-related effects,[21,22] we allow transport coefficients of urea and acid to vary independently and demonstrate that oscillations might be obtained in a urease-loaded cell/membrane providing the transport of acid is greater than that of urea. This situation arises naturally when diffusion of acid is not restricted by the structure of the supporting medium. Bistability, on the other hand, might be observed for both $k_S \geq k_H$ or $k_S < k_H$.

MODEL

The urease catalyzed hydrolysis of urea takes place via the following steps:[20]

Received: February 25, 2014
Revised: April 28, 2014
Published: May 15, 2014

   dx.doi.org/10.1021/jp5019795 | *J. Phys. Chem. B* 2014, 118, 6092−6097

$$CO(NH_2)_2 + H_2O \xrightarrow[R([H^+],[CO(NH_2)_2],[E])]{\text{urease}} 2NH_3 + CO_2$$

$$NH_3 + H^+ \underset{k_{2r}}{\overset{k_2}{\rightleftharpoons}} NH_4^+$$

$$CO_2 + H_2O \underset{k_{3r}}{\overset{k_3}{\rightleftharpoons}} H^+ + HCO_3^-$$

$$HCO_3^- \underset{k_{4r}}{\overset{k_4}{\rightleftharpoons}} CO_3^{2-} + H^+$$

$$H^+ + OH^- \underset{k_{5r}}{\overset{k_5}{\rightleftharpoons}} H_2O \tag{1}$$

where the rate constants are $k_2 = 4.3 \times 10^{10}$ M^{-1} s^{-1}, $k_{2r} = 24$ s^{-1}, $k_3 = 3.7 \times 10^{-2}$ s^{-1}, $k_{3r} = 7.9 \times 10^4$ M^{-1} s^{-1}, $k_4 = 2.8$ s^{-1}, $k_{4r} = 5 \times 10^{10}$ M^{-1} s^{-1}, $k_5 = 10^{11}$ M^{-1} s^{-1}, and $k_{5r} = 10^{-3}$ s^{-1}. For simplicity we write H^+ rather than H_3O^+. With $[H_2O]$ fixed as its concentration is large compared to the other species, these steps result in an eight variable model. Making a few assumptions, detailed in the Appendix, allows the corresponding set of kinetic equations to be reduced into a simple two-variable model where the exchange of matter between the urease-loaded compartment and its surrounding is incorporated as flow terms (Figure 1a). This situation describes the dynamic

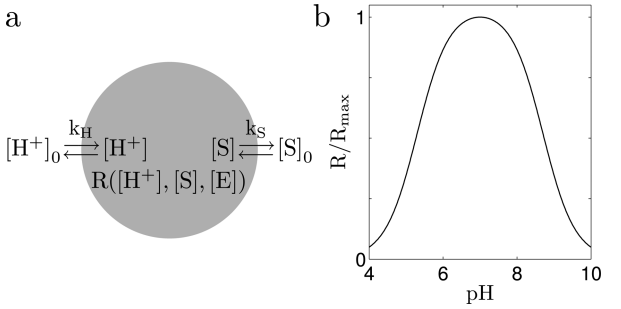

Figure 1. (a) Reaction cell and key processes in the reduced two-variable model of urea hydrolysis: R = enzyme-catalyzed rate, k_H = exchange rate of acid, H^+, and k_S = exchange rate of substrate, S, with external solution of concentrations $[H^+]_0$ and $[S]_0$. (b) Enzyme-catalyzed rate R relative to maximum rate R_{max} as a function of pH.

behavior of a urease-loaded membrane or particle (with the assumption of uniform intracell concentration) as well as a continuous stirred tank reactor (CSTR) in which acid, enzyme and substrate are fed in separately.

$$\frac{d[S]}{dt} = k_S([S]_0 - [S]) - R$$

$$\frac{d[H^+]}{dt} = \left(k_H\left([H^+]_0 - \frac{K_w}{[H^+]_0} - [H^+] + \frac{K_w}{[H^+]}\right) - 2R\right)\left(1 + \frac{K_w}{[H^+]^2}\right)^{-1} \tag{2}$$

where

$$R = \frac{k_E[E][S]}{(K_m + [S])\left(1 + \frac{K_{ES2}}{[H^+]} + \frac{[H^+]}{K_{ES1}}\right)}$$

E, S, and H^+ denote the enzyme urease, the substrate (urea), and the acid, respectively; $[S]_0$ and $[H^+]_0$ are the constant concentrations of the latter two in the reservoir; while $k_E = 3.7 \times 10^{-6}$ mL M u^{-1} s^{-1} (u denotes units as enzyme concentration is given in units/mL so that $k_E[E]$ has the unit of M/s), $K_m = 3 \times 10^{-3}$ M, $K_{ES1} = 5 \times 10^{-6}$ M, $K_{ES2} = 2 \times 10^{-9}$ M are urease specific quantities and $K_w = 10^{-14}$ M^2 is the ion product of water. K_{ES1} and K_{ES2} are the binding constants related to the protonation of the enzyme that lead to the bell-shaped rate-pH curve (Figure 1b). The exchange of substrate and acid molecules through the boundary between the compartment and the reservoir is governed by transport coefficients k_S and k_H, respectively. The transfer rate of acid was varied between $0 < k_H < 0.05$ s^{-1} and substrate: $0 < k_S < 0.09$ s^{-1}.

In order to analyze the dynamic behavior of the two-variable system described by (2) as a function of the transport coefficients, k_H and k_S, we employ linear stability techniques[23] and look at the evolution of small perturbations to the steady state solutions. We focus on finding the criteria required for oscillations and as the first step compute the Jacobian matrix, J, of (2) at steady state values of $[S]_{ss}$ and $[H^+]_{ss}$:

$$J = \begin{pmatrix} \alpha R - k_S & -\beta R \\ 2\alpha\gamma R & -k_H - 2\beta\gamma R \end{pmatrix}_{ss} \tag{3}$$

where

$$\alpha = \frac{-K_m}{K_m[S]_{ss} + [S]_{ss}^2}, \quad \gamma = \left(1 + \frac{K_w}{[H^+]_{ss}^2}\right)^{-1}$$

$$\beta = \left(\frac{K_{ES2}}{[H^+]_{ss}^2} - \frac{1}{K_{ES1}}\right)\left(1 + \frac{[H^+]_{ss}}{K_{ES1}} + \frac{K_{ES2}}{[H^+]_{ss}}\right)^{-1}$$

The eigenvalues $\lambda_{1,2}$ of (3) take the form

$$\lambda_{1,2} = \frac{1}{2}[\mathrm{tr}(J) \pm (\mathrm{tr}(J)^2 - 4\det(J))^{1/2}] \tag{4}$$

where

$$\mathrm{tr}(J) = J_{11} + J_{22} = -(k_H + k_S) + R_{ss}(\alpha - 2\beta\gamma) \tag{5}$$

$$\det(J) = J_{11}J_{22} - J_{12}J_{21} = k_Hk_S + R_{ss}(2k_S\beta\gamma - \alpha k_H) \tag{6}$$

Equations 5 and 6 were solved along with the steady state equations, $d[S]/dt = 0$ and $d[H^+]/dt = 0$, using MATLAB.[24] Numerical simulations of the full model and (2) were performed using XPPAUT[25] with integration method CVODE (the concentrations were scaled in the two variable model, see Appendix) and phase diagrams were produced using AUTO.

RESULTS

Unstable states and oscillations occur for $\mathrm{tr}(J) > 0$ and $\det(J) > 0$. Using these requirements we were able to find the oscillatory domain for a given set of parameters. The values of $\mathrm{tr}(J)$ and $\det(J)$ are plotted in Figure 2 as a function of the substrate exchange rate k_S with k_H fixed. The trace and determinant are positive within the range of 0.00293 $s^{-1} < k_S < 0.00375$ s^{-1}. The pH oscillations obtained in numerical simulations of (2) are shown in Figure 2b.

In Figure 3, we present phase diagrams in the k_S–k_H plane for two different sets of parameters. Oscillations, bistability, or a single steady state (low or high pH) are obtained as k_H and k_S

dx.doi.org/10.1021/jp5019795 | J. Phys. Chem. B 2014, 118, 6092–6097

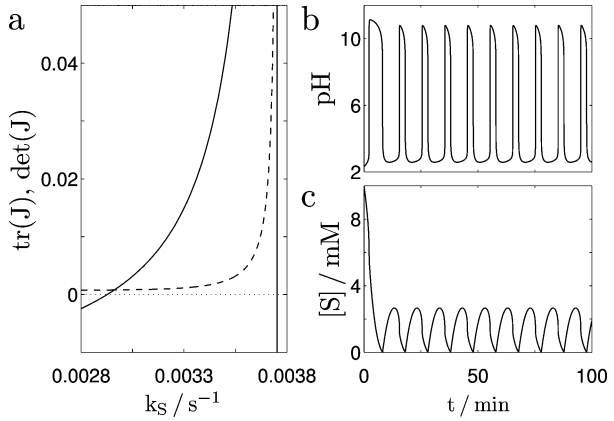

Figure 2. (a) Trace, tr(J), (solid line) and determinant, det(J), (dashed line) versus exchange rate k_S with $[S]_0$ = 10 mM, $[H^+]_0$ = 5 mM, [E] = 6000 u/mL and k_H = 0.015 s^{-1}; det(J) was multiplied by 10 for clarity. The Hopf bifurcation points occur where tr(J) = 0 and give the limits of k_S required for oscillations. Oscillations, when k_S = 0.0032 s^{-1}, in (b) pH and (c) substrate.

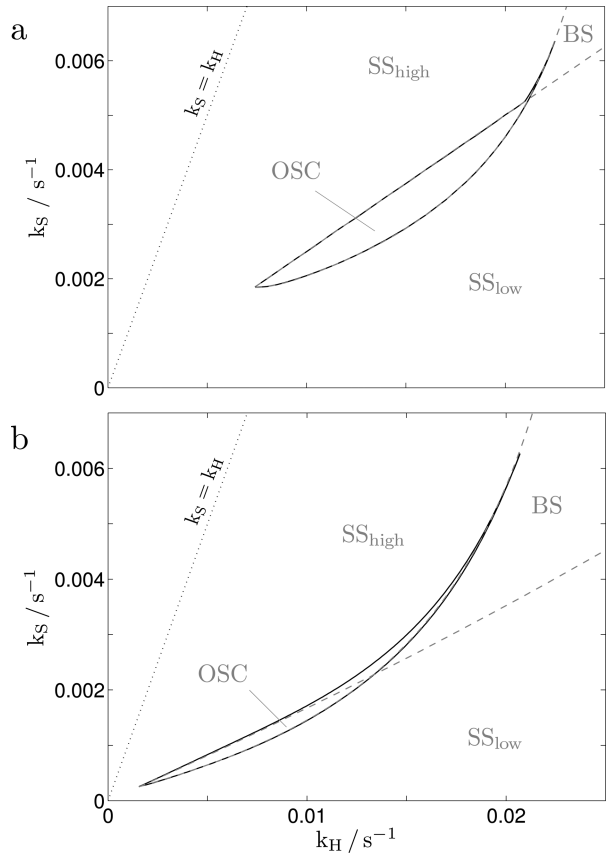

Figure 3. Phase diagrams in $k_S - k_H$ space for two sets of parameters: (a) $[S]_0$ = 10 mM, $[H^+]_0$ = 5 mM, [E] = 6000 u/mL; (b) $[S]_0$ = 0.4 mM, $[H^+]_0$ = 0.13 mM, [E] = 30 u/mL. Limit cycles are predicted to exist by theory (tr(J) > 0 and det(J) > 0) within the solid lines. Domains marked by dashed lines separate the regions of oscillations, OSC, steady states, SS (low and high pH), and the bistable regime, BS, obtained using AUTO.

are varied. We found that the regions of oscillations determined by the linear stability theory overlapped those mapped out using AUTO. For both sets of parameters, oscillations occur if $k_S < k_H$.

To establish if oscillations in the urea−urease system exist only when this relation holds we supposed that $k_H \leq k_S$ and examined the requirements: tr(J) > 0 and det(J) > 0, which yielded

$$k_H \leq k_S < R_{ss}(\alpha - 2\beta\gamma) - k_H \tag{7}$$

and

$$k_H \leq k_S < \frac{\alpha k_H R_{ss}}{k_H + 2\beta\gamma R_{ss}} \tag{8}$$

respectively. Rearrangement leads to a pair of mutually exclusive inequalities:

$$R_{ss}(\alpha - 2\beta\gamma) \geq 2k_H \tag{9}$$

$$R_{ss}(a - 2\beta\gamma) \leq k_H \tag{10}$$

confirming that oscillations, indeed, may occur for $k_S < k_H$ only. This result may apply for any enzyme-catalyzed reaction producing n moles of basic product (see Appendix).

Although oscillations are not possible for $k_H \leq k_S$, it is clear from earlier work that bistability can occur if $k_H = k_S$. The phase diagram in Figure 3b is plotted for larger values of k_H and k_S in Figure 4 and the region of bistability is seen to extend over a wide range of k_H/k_S, including $k_S > k_H$.

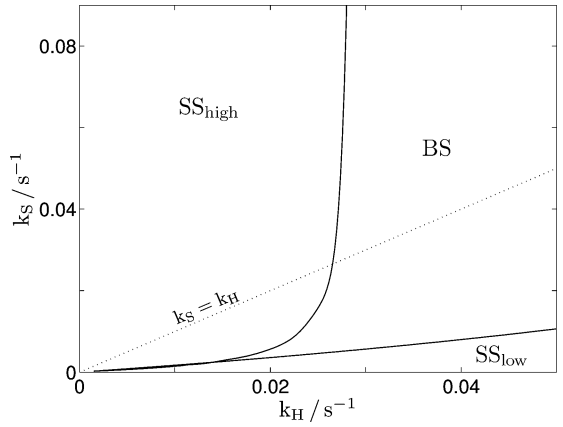

Figure 4. Phase diagram in $k_S - k_H$ space for $[S]_0$ = 0.4 mM, $[H^+]_0$ = 0.13 mM, [E] = 30 u/mL illustrating that the region of bistability crosses the $k_H = k_S$ line.

The enzyme and substrate concentrations that give rise to oscillations are obtained for fixed k_H/k_S = 6.4 in numerical simulations of the two variable model and compared to the full, eight variable model in Figure 5. Oscillations are observed for a smaller, but nevertheless significant range of [E] and $[S]_0$ in the full model. The oscillations in pH are also smaller in amplitude in the full model.

Bifurcation diagrams are plotted in Figure 5 for three different enzyme concentrations in the two variable model. At high enzyme concentration, as the substrate concentration is increased a transition is observed from low to high pH with a relatively sharp change in pH over a small range of substrate concentration (Figure 5b). At intermediate enzyme concentrations, a subcritical Hopf bifurcation occurs and large amplitude oscillations are observed between pH = 4 and pH = 9 over a narrow range of substrate concentrations (Figure 5c). For low enzyme concentrations, bistability between pH 4

dx.doi.org/10.1021/jp5019795 | J. Phys. Chem. B 2014, 118, 6092−6097

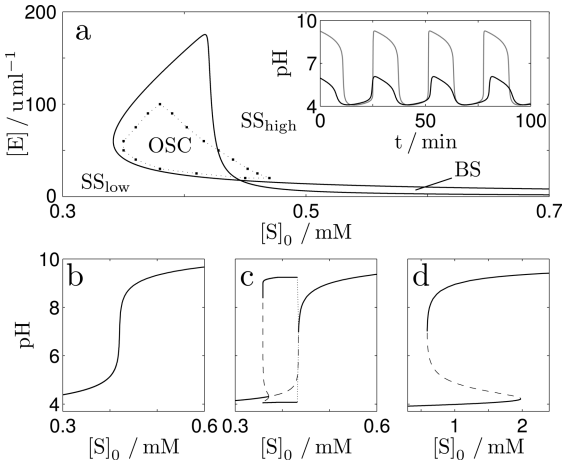

Figure 5. (a) Phase diagram in $[E]_0 - [S]_0$ space obtained in the two-variable model with $[H^+]_0 = 0.13$ mM, $k_H = 0.009\ s^{-1}$, $k_S = 0.0014\ s^{-1}$ where OSC = oscillatory, BS = bistable, SS_{high} = high pH steady state and SS_{low} = low pH steady state. The points connected by a dotted line show the region of oscillations obtained in the full eight-variable model of urea hydrolysis (See (A1) in Appendix) for the same parameters (with the loss rate $k = 0.0014\ s^{-1}$ and exchange rate $k_{OH} = 0.0045\ s^{-1}$). The inset compares oscillations in the full model (small amplitude) with the two-variable model. (b–d) pH – $[S]_0$ bifurcation diagrams obtained in the two-variable model with $[E]_0$ = (b) 200, (c) 30, and (d) 3 u/mL.

and 9 occurs over a wide range of substrate concentrations (Figure 5d).

DISCUSSION

Differential transport arises naturally in cells as a result of variations in the permeability of the cell membrane to different species. The combination of an autocatalytic process and differential transport was already suggested to give rise to stationary patterns and oscillations in 1952 in the seminal theoretical work of Turing on the chemical basis of morphogenesis.[26] In his coupled cell model, the transport of the autocatalytic species was slower than the other, inhibitory, species: this condition for pattern formation is often referred to as long-range inhibition, short-range activation.[27] Turing's work has inspired intensive research but there is still limited evidence of such processes underlying pattern formation in biology.[28]

The formation of non-neutral products in enzyme catalyzed reactions can lead to rate-acceleration as these reactions typically display bell-shaped rate-pH curves. This mechanism of feedback was proposed to play a key role in pH oscillations obtained in a computational model involving a membrane-bound enzyme, papain, and diffusion of substrate, an ester, from the surrounding solution.[1] In the model, acid was produced and the diffusion coefficient of acid was five times larger than the other species. While the chemical nature of the feedback has been analyzed,[10,29] the importance of the inherent differential transport was perhaps under-emphasized in earlier work and there is sparse experimental evidence of oscillations in the papain reaction.

The urea–urease reaction occurs in numerous cellular systems and is used by bacteria in order to raise the local pH.[15] In this reaction, the production of ammonia leads to a decrease in acid and hence rate acceleration as the acid concentration decreases. The reaction has the distinct advantages of high solubility and stability of substrate and enzyme in water making it suitable for experiments *in vitro*. Propagating pH wavefronts have been observed when the reaction was performed in thin layers[20] and bistability between a low and high pH state were obtained in a continuous stirred tank reactor (CSTR) when sulfuric acid and enzyme were pumped in separately from urea.[19]

In order to determine the conditions for oscillations in the urea–urease reaction, a two-variable model was derived in which acid and substrate, urea, are supplied at rates k_H and k_S from an external medium to an enzyme-containing cell. The results in the two variable model were qualitatively reproduced in simulations of the full, eight variable, model given in earlier work[19,20] and the concentrations of species compared well with those used in experiments. Oscillations were observed between pH 4 and 6 in the full model. Thus, the reaction appears a good candidate for the observation of oscillations in experiments, providing the necessary condition that $k_H > k_S$ is met.

The model describes the reaction taking place in an enzyme-loaded compartment; however the results presented here have an important implication: no oscillations can develop in the urea–urease reaction in a CSTR for which the flow rate $F = k_S = k_H$. In spatially distributed aqueous phase reactions, the diffusion coefficient of acid is typically much greater than that of the other species and depends on the ionic strength of the solution and other factors.[30] With diffusion coefficients, $D_H = 5–9 \times 10^{-3}\ mm^2\ s^{-1}$ and $D_S = 1.4 \times 10^{-3}\ mm^2\ s^{-1}$, the ratio of D_H/D_S may vary between 4 and 6, which compares well with the ratios of transport rates for oscillations shown in Figure 3 and the value of 6.4 used to obtain Figure 5.

Differential diffusion was also found to induce oscillations in the chlorite–tetrathionate,[31] Landolt,[32] and iodate–arsenous acid[33] reactions and in a model of a single step cubic autocatalytic process,[34] all exhibiting bistability only in a CSTR. In these systems, the spatially nonuniform steady state is destabilized by the long-range activation through the enhanced depletion of the autocatalyst due to its fast diffusion compared to the rest of the species. The resulting oscillations develop in a domain extending from the bistable regime. Similarly, the regions of bistability and oscillations are connected in the urea–urease system with oscillations occurring only if the exchange rate of acid is sufficiently higher than that of the other species. Without the required difference in exchange rates the high pH steady state replaces the otherwise present oscillations, indicating that in the urea–urease system the fast replenishment of acid is the destabilizing process needed for oscillations to develop.

The transport of urea and other species into *Helicobacter pylori* involves proton-gated membrane channels and continues to be the subject of investigation.[35] It would be of interest to develop a model that included pH-dependent transport rates of species and determine their influence on the dynamic behavior reported here. Bacteria emit autocatalytic species in order to synchronize their activity in a phenomenon known as quorum sensing.[36] It remains to be seen whether autocatalysis driven by urease contributes to the survival of *H. pylori* in the stomach.

APPENDIX

The rate equations corresponding to the full mechanism given by (1) in an open reactor or enzyme loaded particle are

dx.doi.org/10.1021/jp5019795 | J. Phys. Chem. B 2014, 118, 6092–6097

$$\begin{aligned}
\frac{d[CO(NH_2)_2]}{dt} &= -R + k_S([CO(NH_2)_2]_0 - [CO(NH_2)_2])\\
\frac{d[NH_3]}{dt} &= 2R + k_{2r}[NH_4^+] - k_2[NH_3][H^+] - k[NH_3]\\
\frac{d[NH_4^+]}{dt} &= k_2[NH_3] - k_{2r}[NH_4^+][H^+] - k[NH_4^+]\\
\frac{d[CO_2]}{dt} &= R + k_3[H^+][HCO_3^-] - k_{3r}[CO_2] - k[CO_2]\\
\frac{d[HCO_3^-]}{dt} &= k_{3r}[CO_2] - k_3[HCO_3^-][H^+] - k_{4r}[HCO_3^-]\\
&\quad + k_4[CO_3^{2-}][H^+] - k[HCO_3^-]\\
\frac{d[CO_3^{2-}]}{dt} &= k_{4r}[HCO_3^-] - k_4[CO_3^{2-}][H^+] - k[CO_3^{2-}]\\
\frac{d[H^+]}{dt} &= k_{5r} - k_5[H^+][OH^-] + k_{4r}[HCO_3^-]\\
&\quad - k_4[CO_3^{2-}][H^+] + k_{3r}[CO_2]\\
&\quad - k_3[HCO_3^-][H^+] + k_{2r}[NH_4^+]\\
&\quad - k_2[NH_3][H^+] + k_H([H^+]_0 - [H^+])\\
\frac{d[OH^-]}{dt} &= k_{5r} - k_5[H^+][OH^-] + k_{OH}([OH^-]_0 - [OH^-])
\end{aligned} \tag{A1}$$

where k denotes the loss rate of chemical species (assuming there is no carbon dioxide or ammonia in the inflow solution) and k_S, k_H and k_{OH} are the exchange rates of S, H^+, and OH^- respectively (with inflow concentrations given in the main text). The loss and exchange rates used in the simulations of the full model are given in the figure caption of Figure 5.

Neglecting the production of CO_2 as it plays a small role in the dynamics, eq A1 reduces into

$$\begin{aligned}
&S \xrightarrow[R([H^+],[S],[E])]{\text{enzyme}} 2P\\
&P + H^+ \underset{k_{2r}}{\overset{k_2}{\rightleftharpoons}} PH^+\\
&H^+ + OH^- \underset{k_{5r}}{\overset{k_5}{\rightleftharpoons}} H_2O
\end{aligned} \tag{A2}$$

where, for simplicity, S, P, and PH^+ denote the substrate urea, ammonia, and ammonium, respectively. The corresponding set of kinetic equations for a membrane or particle is

$$\frac{d[S]}{dt} = k_S([S]_0 - [S]) - R \tag{A3}$$

$$\frac{d[P]}{dt} = 2R - k_2[P][H^+] + k_{2r}[PH^+] - k[P] \tag{A4}$$

$$\frac{d[PH^+]}{dt} = k_2[P][H^+] - k_{2r}[PH^+] - k[PH^+] \tag{A5}$$

$$\begin{aligned}
\frac{d[H^+]}{dt} &= k_{5r} - k_5[H^+][OH^-] + k_{2r}[PH^+] - k_2[P][H^+]\\
&\quad + k_H([H^+]_0 - [H^+])
\end{aligned} \tag{A6}$$

$$\begin{aligned}
\frac{d[OH^-]}{dt} &= k_{5r} - k_5[H^+][OH^-]\\
&\quad + k_{OH}([OH^-]_0 - [OH^-])
\end{aligned} \tag{A7}$$

Compared with the rate of the enzymatic step, the equilibrium between H_2O, H^+ and OH^- is assumed to be established instantaneously. Hence, we substitute $[OH^-] = K_w/[H^+]$ into eq A7 which converts the left−hand side into

$$\frac{d[OH^-]}{dt} = \frac{d(K_w/[H^+])}{d[H^+]}\frac{d[H^+]}{dt} = -\frac{K_w}{[H^+]^2}\frac{d[H^+]}{dt}$$

Then subtracting eq A7 from eq A6 and, for convenience, assuming that $k_H = k_{OH}$ yields

$$\begin{aligned}
\frac{d[H^+]}{dt} &= \left(k_H\left([H^+]_0 - \frac{K_w}{[H^+]_0} - [H^+] + \frac{K_w}{[H^+]}\right)\right.\\
&\quad \left. + k_{2r}[PH^+] - k_2[P][H^+]\right)\left(1 + \frac{K_w}{[H^+]^2}\right)^{-1}
\end{aligned} \tag{A8}$$

We find that the $[PH^+]$ in the full model can be approximated by its steady state value i.e. $[PH^+] = k_2[P][H^+]/(k_{2r} + k)$, and that the loss of P to the surrounding solution, $-k[P]$ in eq A4, can be neglected on the basis of $k \ll k_2[H^+]$ in the combined removal term $-(k_2[H^+] + k)[P]$, which remains true even for conditions seen in Figure 4. By now applying the dynamic steady state approximation to $[P]$, eq A4 becomes

$$-k_2[P][H^+] + k_{2r}[PH^+] = -2R$$

which following substitution into eq A8 and along with eq A3 henceforth gives the two variable model, (2).

The model was scaled for convenience using $y = [H^+]/K_{ES1}$ and $x = [S]/K_m$ and thus obtaining the following for simulations in XPPAUT:

$$\frac{dx}{dt} = k_S(x_0 - x) - \frac{R}{K_m} \tag{A9}$$

$$\frac{dy}{dt} = \left(k_H\left(y_0 - \frac{K_w}{y_0 K_{ES1}^2} - y + \frac{K_w}{yK_{ES1}^2}\right) - \frac{2R}{K_{ES1}}\right)A^{-1} \tag{A10}$$

where

$$R = \frac{k_E[E]x}{(1 + K_{ES2}(yK_{ES1})^{-1} + y)(1 + x)},$$

$$A = 1 + \frac{K_w}{y^2 K_{ES1}^2}$$

We would like to note that in (3) J_{22} can be simplified from its precise expression

$$J_{22} = (-k_H - 2\beta\gamma R - 2\gamma' R + \gamma'\delta k_H)_{ss}$$

where

$$\gamma' = \frac{d\gamma}{d[H^+]} = 2K_w[H^+]_{ss}^{-3}\left(1 + \frac{K_w}{[H^+]_{ss}^2}\right)^{-2},$$

$$\delta = \left([H^+]_0 - \frac{K_w}{[H^+]_0} - [H^+]_{ss} + \frac{K_w}{[H^+]_{ss}}\right)$$

by realizing that $-\gamma'(2R - \delta k_H) = 0$ because the bracketed term is zero at the steady state.

dx.doi.org/10.1021/jp5019795 | J. Phys. Chem. B 2014, 118, 6092−6097

In generalizing the urea−urease system one may consider the following steps:

$$\mathrm{S} \xrightarrow[\mathrm{R}([\mathrm{H}^+],[\mathrm{S}],[\mathrm{E}])]{\text{enzyme}} n\mathrm{P}$$

$$\mathrm{P} + \mathrm{H}^+ \underset{k_{2r}}{\overset{k_2}{\rightleftharpoons}} \mathrm{PH}^+$$

$$\mathrm{H}^+ + \mathrm{OH}^- \underset{k_{Sr}}{\overset{k_S}{\rightleftharpoons}} \mathrm{H_2O} \qquad \text{(A11)}$$

involving an enzymatic process in which each substrate molecule is transformed into n basic product molecules. It can be shown that in this generalized system oscillations may occur if $\mathrm{tr}(J) = -(k_H + k_S) + R_{ss}(\alpha - n\beta\gamma) > 0$ and $\det(J) = k_H k_S + R_{ss}(nk_S\beta\gamma - \alpha k_H) > 0$, and that these requirements cannot be fulfilled when $k_H \leq k_S$ for which they rearrange to $R_{ss}(\alpha - n\beta\gamma) \geq 2k_H$ and $R_{ss}(\alpha - n\beta\gamma) \leq k_H$, respectively.

AUTHOR INFORMATION

Corresponding Author

*(T.B.) E-mail: T.Bansagi@leeds.ac.uk.

Notes

The authors declare no competing financial interest.

ACKNOWLEDGMENTS

T.B. was supported by a Marie Curie International Incoming Fellowship (grant agreement PIIF-GA-2010-274677).

REFERENCES

(1) Caplan, S. R.; Naparstek, A.; Zabusky, N. J. Chemical oscillations in a membrane. *Nature* **1973**, *245*, 364−366.

(2) Hahn, H.-S.; Nitzan, A.; Ortoleva, P.; Ross, J. Threshold excitations, relaxation oscillations, and effect of noise in an enzyme reaction. *Proc. Natl. Acad. Sci. U. S. A.* **1974**, *71*, 4067−4071.

(3) Zabusky, N.; Hardin, R. Phase transition, stability, and oscillations for an autocatalytic, single, first-order reaction in a membrane. *Phys. Rev. Lett.* **1973**, *31*, 812−815.

(4) Chay, T. R. A model for biological oscillations. *Proc. Natl. Acad. Sci. U. S. A.* **1981**, *78*, 2204−2207.

(5) Goldbeter, A.; Caplan, S. R. Oscillatory enzymes. *Annu. Rev. Biophys. Bioeng.* **1976**, *5*, 449−476.

(6) Naparstek, A.; Thomas, D.; Roy Caplan, S. An experimental enzyme-membrane oscillator. *Biochim. Biophys. Acta (BBA)-Biomembranes* **1973**, *323*, 643−646.

(7) Temminck Groll, J. Periodische Erscheinungen bei Fermenten als Folge ihrer kolloiden Beschaffenheit. *Colloid Polym. Sci.* **1917**, *21*, 138−148.

(8) Friboulet, A.; Thomas, D. Electrical excitability of artificial enzyme membranes: III. Hysteresis and oscillations observed with immobilized acetylcholinesterase membranes. *Biophys. Chem.* **1982**, *16*, 153−157.

(9) Goldbeter, A. Oscillatory enzyme reactions and Michaelis−Menten kinetics. *FEBS Lett.* **2013**, *587*, 2778−2784.

(10) Shen, P.; Larter, R. Role of substrate inhibition kinetics in enzymatic chemical oscillations. *Biophys. J.* **1994**, *67*, 1414−1428.

(11) Ohmori, T.; Nakaiwa, M.; Yamaguchi, T.; Kawamura, M.; Yang, R. Y. Self-sustained pH oscillations in a compartmentalized enzyme reactor system. *Biophys. Chem.* **1997**, *67*, 51−57.

(12) Zagora, J.; Voslař, M.; Schreiberová, L.; Schreiber, I. Excitability in chemical and biochemical pH-autocatalytic systems. *Faraday Discuss.* **2002**, *120*, 313−324.

(13) Ohmori, T.; Yang, R. Y. Self-sustained pH oscillations in immobilized proteolytic enzyme systems. *Biophys. Chem.* **1996**, *59*, 87−94.

(14) Vanag, V. K.; Míguez, D. G.; Epstein, I. R. Designing an enzymatic oscillator: Bistability and feedback controlled oscillations with glucose oxidase in a continuous flow stirred tank reactor. *J. Chem. Phys.* **2006**, *125*, 194515−194515.

(15) Stingl, K.; Altendorf, K.; Bakker, E. P. Acid survival of Helicobacter pylori: how does urease activity trigger cytoplasmic pH homeostasis? *Trends Microbiol.* **2002**, *10*, 70−74.

(16) Olsen, L. F.; Andersen, A. Z.; Lunding, A.; Brasen, J. C.; Poulsen, A. K. Regulation of Glycolytic Oscillations by Mitochondrial and Plasma Membrane H^+-ATPases. *Biophys. J.* **2009**, *96*, 3850−3861.

(17) Beg, A. A.; Ernstrom, G. G.; Nix, P.; Davis, M. W.; Jorgensen, E. M. Protons Act as a Transmitter for Muscle Contraction in *C. elegans*. *Cell* **2008**, *132*, 149−160.

(18) Mobley, H. L.; Mendz, G. L.; Hazell, S. L. *Restriction and Modification Systems−Helicobacter pylori: Physiology and Genetics*; ASM press: 2001.

(19) Hu, G.; Pojman, J. A.; Scott, S. K.; Wrobel, M. M.; Taylor, A. F. Base-catalyzed feedback in the urea-urease reaction. *J. Phys. Chem. B* **2010**, *114*, 14059−14063.

(20) Wrobel, M. M.; Bánsági, T., Jr.; Scott, S. K.; Taylor, A. F.; Bounds, C. O.; Carranzo, A.; Pojman, J. A. PH wave-front propagation in the urea-urease reaction. *Biophys. J.* **2012**, *103*, 610−615.

(21) Chay, T. R. Proton transport across charged membrane and pH oscillations. *Biophys. J.* **1980**, *30*, 99−118.

(22) Chay, T. R.; Zabusky, N. J. Dual-mode potential oscillations on an immobilized acetylcholinesterase membrane system. *J. Biol. Phys.* **1983**, *11*, 27−33.

(23) Gray, P.; Scott, S. K. *Chemical oscillations and instabilities: non-linear chemical kinetics*; Clarendon Press. Oxford University Press: 1990.

(24) MATLAB, *version 7.12.0 (R2011a)*; The MathWorks Inc.: Natick, MA, 2011.

(25) Ermentrout, B. *Simulating, analyzing, and animating dynamical systems: a guide to XPPAUT for researchers and students*; Siam: 2002; Vol. *14*.

(26) Turing, A. The Chemical Basis of Morphogenesis. *Philos. Trans. R. Soc. B* **1952**, *237*, 37−72.

(27) Meinhardt, H. *Models of biological pattern formation*; Academic Press: London, 1982; Vol. *6*.

(28) Maini, P. K.; Woolley, T. E.; Baker, R. E.; Gaffney, E. A.; Lee, S. S. Turing's model for biological pattern formation and the robustness problem. *Interface Focus* **2012**, *2*, 487−496.

(29) Schreiber, I.; Hung, Y.-F.; Ross, J. Categorization of some oscillatory enzymatic reactions. *J. Phys. Chem.* **1996**, *100*, 8556−8566.

(30) Cussler, E. L. *Diffusion: mass transfer in fluid systems*; Cambridge university press: 2009.

(31) Fuentes, M.; Kuperman, M.; Boissonade, J.; Dulos, E.; Gauffre, F.; De Kepper, P. Dynamical effects induced by long range activation in a nonequilibrium reaction-diffusion system. *Phys. Rev. E* **2002**, *66*, 056205.

(32) Boissonade, J.; De Kepper, P. Multiple types of spatio-temporal oscillations induced by differential diffusion in the Landolt reaction. *Phys. Chem. Chem. Phys.* **2011**, *13*, 4132−4137.

(33) Benyaich, K.; Erneux, T.; Métens, S.; Villain, S.; Borckmans, P. Spatio-temporal behaviors of a clock reaction in an open gel reactor. *Chaos: An Interdisciplinary Journal of Nonlinear Science* **2006**, *16*, 037109.

(34) Szalai, I. Linear diffusive feed approach to explaining long range activation induced oscillations. *Reaction Kinetics, Mechanisms and Catalysis* **2014**, *111*, 431−442.

(35) Strugatsky, D.; McNulty, R.; Munson, K.; Chen, C.-K.; Soltis, S. M.; Sachs, G.; Luecke, H. Structure of the proton-gated urea channel from the gastric pathogen Helicobacter pylori. *Nature* **2012**, *493*, 255−258.

(36) Miller, M. B.; Bassler, B. L. Quorum sensing in bacteria. *Annu. Rev. Microbiol.* **2001**, *55*, 165−199.